Low frequency sound propagation in activated carbon

F. Bechwati and M. R. Avis
Acoustics Research Centre, University of Salford, Salford, M5 4WT, United Kingdom

D. J. Bull
Institute for Materials Research, University of Salford, Salford, M5 4WT, United Kingdom

T. J. Cox[a] and J. A. Hargreaves
Acoustics Research Centre, University of Salford, Salford, M5 4WT, United Kingdom

D. Moser and D. K. Ross
Institute for Materials Research, University of Salford, Salford, M5 4WT, United Kingdom

O. Umnova and R. Venegas
Acoustics Research Centre, University of Salford, Salford, M5 4WT, United Kingdom

(Received 25 October 2011; revised 26 April 2012; accepted 28 April 2012)

Activated carbon can adsorb and desorb gas molecules onto and off its surface. Research has examined whether this sorption affects low frequency sound waves, with pressures typical of audible sound, interacting with granular activated carbon. Impedance tube measurements were undertaken examining the resonant frequencies of Helmholtz resonators with different backing materials. It was found that the addition of activated carbon increased the compliance of the backing volume. The effect was observed up to the highest frequency measured (500 Hz), but was most significant at lower frequencies (at higher frequencies another phenomenon can explain the behavior). An apparatus was constructed to measure the effective porosity of the activated carbon as well as the number of moles adsorbed at sound pressures between 104 and 118 dB and low frequencies between 20 and 55 Hz. Whilst the results were consistent with adsorption affecting sound propagation, other phenomena cannot be ruled out. Measurements of sorption isotherms showed that additional energy losses can be caused by water vapor condensing onto and then evaporating from the surface of the material. However, the excess absorption measured for low frequency sound waves is primarily caused by decreases in surface reactance rather than changes in surface resistance.
 [http://dx.doi.org/10.1121/1.4725761]

PACS number(s): 43.55.Ev [NX] Pages: 239–248

I. INTRODUCTION

Research into how sound interacts with activated carbons was initiated following suggestions that using activated carbon in loudspeaker enclosures provides "compliance enhancement,"[1] thus enabling smaller loudspeaker cabinets to be used while preserving reproduction bandwidth. Activated carbon is a material that exhibits adsorbing and desorbing properties. Adsorption occurs when molecules from a surrounding gas are attracted to a material's microstructure and held in place on the surface by van der Waals forces (weak physical-attraction forces); desorption is the opposite process. Activated carbons possess a complex porous structure, with a large internal surface area, and a considerable adsorption capacity caused by free electrons in the deformed graphene layers.

This paper is concerned with examining the significance of sorption effects to acoustic waves, as sound propagates through activated carbon. The sorption of activated carbon has been very extensively studied, but usually using pressures that are far in excess of those found in typical audible sound waves. The dynamic pressure fluctuations that occur with sound waves are very different than the static pressures commonly used in activated carbon studies. Furthermore, activated carbon has a complex microstructure, which makes it difficult to determine whether it is sorption or another phenomenon that explains the compliance enhancement.

The proposition being tested is that there are two physical phenomena associated with sorption that accompany sound propagation through activated carbon at low frequencies: (1) An increase in bulk volume compliance caused by a change in the effective density of the interacting gas, and (2) an increase in energy loss due to the sorption cycle. (The term "effective" is used to signify that this is the density experienced by the acoustic waves rather than the more normal definition of mass divided by volume.)

Consequently, one aim of this paper is to present measurements quantifying any increase in volume compliance caused by activated carbon, and furthermore, to explore whether the increase is due to changes in gas density caused by sorption. However, if gas molecules undergo a cyclical process of adsorption and desorption caused by the compressions and rarefactions of a sound wave, then the process should be associated with energy loss, caused by effects such as transfer of heat between the adsorbate molecules and

[a]Author to whom correspondence should be addressed. Electronic mail: t.j.cox@salford.ac.uk

the adsorbent surface, and energy lost in condensation. An investigation into energy losses forms another focus of this paper.

This was an experimental study. Section II describes surface impedance measurements for Helmholtz resonators incorporating activated carbon. These reveal significant downward shifts in resonant frequencies compared to devices with an empty backing volume or non-adsorbent granular material in the backing volume. Section III describes a new method for determining the effective porosity of a material exhibiting adsorption for low frequency acoustic pressures. The apparatus also provides evidence for whether sorption is significant to sound propagation. Section IV presents results for the surface impedance of activated carbon to quantify the energy losses within the material. Section V presents results of isotherm measurements which investigate the sorption process and quantifies the activated carbon being examined. This is important because the properties of activated carbon vary greatly depending on how it is made, and only some carbons display strong effects with sound waves.

II. MEASUREMENT OF HELMHOLTZ RESONATORS

The surface impedance of various Helmholtz resonators with different backing conditions was measured in an impedance tube allowing the compliance of an acoustic enclosure to be examined up to 500 Hz.

A large impedance tube designed to work at low frequencies was constructed as shown in Fig. 1. The device was built from mild steel tubing, circular in cross section with an inner diameter of 324 mm and walls 22 mm thick. At the lower end, a sample holder was constructed from the same tube material, with a rigid termination provided by 50 mm thick medium density fiberboard. The tube was excited using a 30 cm loudspeaker driver mounted in a wooden box at the opposite end.

The impulse response at each of the four microphones was measured using a swept sine signal. An adaptation of the standard transfer function method was used to derive the surface impedance.[2] Various transfer functions are computed between all four microphones so as to cover the required measurement bandwidth, and a modified version of a least-squares optimization method used to derive the surface impedance.[3,4] As part of the commissioning process, measurements of a mineral wool sample in the new apparatus were compared to measurements of the sample in a smaller, conventional impedance tube and shown to be the same where the measurement bandwidths overlapped.

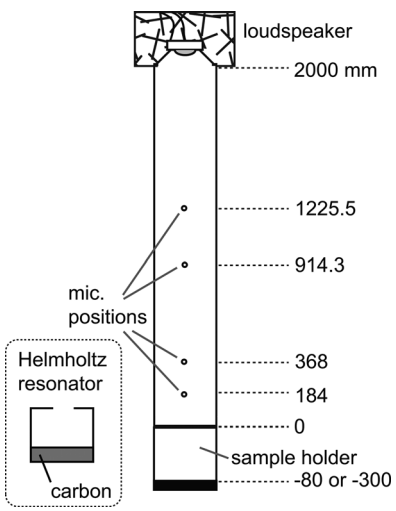

FIG. 1. Bass impedance tube, and inset showing one of the Helmholtz resonators.

TABLE I. The number of apertures, radius, and open areas for the Helmholtz resonators measured.

One aperture	Radius (mm)	7.7	11.5	15.6	20.5	26.3	32.5	39.7	47.7
	Open area (%)	0.23	0.50	0.93	1.6	2.64	4.03	6.01	8.67
Two apertures	Radius (mm)	25	30	35	40	45	50	55	60
	Open area (%)	4.76	6.85	9.33	12.2	15.4	19.1	23.1	27.4

To give a range of resonant frequencies, a variety of Helmholtz resonators were built. The backing volume and length of the aperture neck were fixed at 5768 cm^3 and 12 mm, respectively. Table I shows the different plate geometries used.

Two different porous materials were placed at the bottom of the backing volume; densely packed grains of sand and activated carbon. Measurements are also compared to the case of an empty backing volume. The two porous materials were sieved for a grain size distribution between 0.30 and 0.42 mm. The samples measured 2000 cm^3 in volume, which formed a layer 2.42 cm thick in the backing volume. Sieved sand was chosen as a comparison material because it is assumed that for a given grain size distribution and packing condition, sand and granular activated carbon will have a similar intergranular structure (but very different microscale and mesoscale in-grain porosity).

A. Results

Figure 2 shows surface impedance spectra for three of the resonators (each having a different resonant frequency) for the three backing conditions tested. The real part of the surface impedance is larger for activated carbon than sand; this will be discussed later. Of immediate interest is the imaginary part of the surface impedance. The addition of sand to the backing volume increases the resonant frequency by reducing the free air volume, as often happens with a conventional Helmholtz resonator. The addition of a similar volume of activated carbon, on the other hand, decreases the resonant frequency.

Figure 3 plots the resonant frequencies for all devices tested confirming the above-described trends in resonant frequencies. The increase in backing volume compliance achieved by the activated carbon sample is most pronounced at low frequency (maximum 35% reduction in resonant frequency), with the effect becoming less pronounced above 315 Hz. However, a comparison between results for sand and activated carbon reveals that even at the highest frequency tested (500 Hz), the resonant frequency is 20 Hz lower for activated carbon than sand (a 4% reduction).

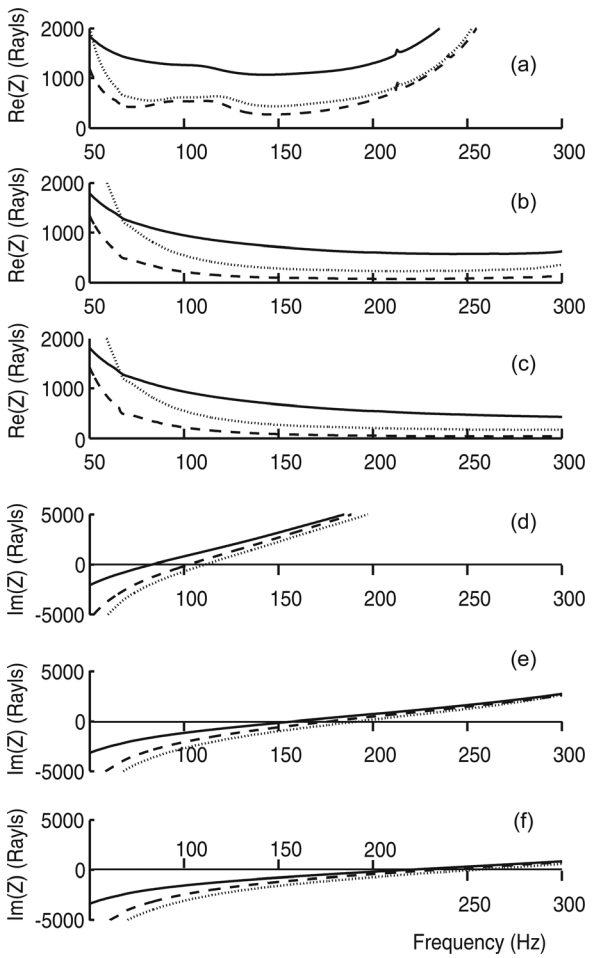

FIG. 2. Measured real and imaginary surface impedance (Z) for three of the resonators and three different backing conditions: ___, empty; ___, activated carbon; and ....., sand. (a) Re(Z) resonator I; (b) Re(Z) resonator II; (c) Re(Z) resonator III; (d) Im(Z) resonator I; (e) Im(Z) resonator II; (f) Im(Z) resonator III.

The resonators with sand or activated carbon have two acoustic media in their backing volume—a layer of porous absorbent behind a layer of air. In contrast to the adiabatic behavior expected for the empty sample backing volume and air layers, the saturating air within the porous absorbent may be assumed to behave isothermally. Since the isothermal bulk modulus is lower than the adiabatic bulk modulus, the system can have a lower resonant frequency even without adsorption. Selamet *et al.*[5] implicitly demonstrated this with measurements and predictions on a silencer system. For the thickness of absorbent most comparable to our activated carbon measurements, Selamet *et al.* found a shift in resonant frequency of 5%–8%. Consequently, the shift at higher frequencies with activated carbon can be explained without adsorption. The larger shifts at lower frequencies, however, warrant further investigation.

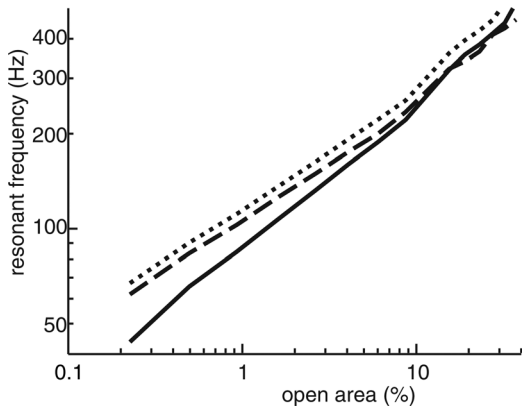

FIG. 3. Resonant frequencies for the Helmholtz resonators vs open area of the top plate with three backing conditions: ___, empty; ___, activated carbon; and ....., sand.

III. MEASUREMENT OF SORPTION KINETICS USING SOUND WAVES

A new apparatus to quantify and examine adsorption using sound waves was developed. Analyzing measurements from the new apparatus use formulations that include adsorption processes, providing evidence as to whether adsorption is a significant phenomenon at audio pressures and frequencies.

A sample of activated carbon is placed in a sealed container. The volume of the container can be changed dynamically by small amounts using a sealed loudspeaker driver driven at low frequency. The volume of the container is changed by a known amount and the pressure change is measured. If sorption occurs, the pressure amplitude will be reduced from that expected by a naive application of ideal gas equations, because during compression the number of moles in the gaseous phase decreases because some of the gas adsorbs (and condenses) onto the surface of the activated carbon (and during rarefaction the opposite effect occurs). By making measurements at different volume displacements, it is possible to derive the effective porosity. The effective porosity should be greater than one, because the activated carbon presents an apparent air volume to sound waves that is greater than its physical air volume. Furthermore, because adsorption is a process that takes time, it is also possible to look at the phase of the acoustic pressure relative to the dynamic displacement, and further examine whether adsorption is important.

Figure 4 shows the measurement apparatus. A 2 in. loudspeaker (with a very rigid cone) provided the volume change and its displacement was monitored by a B&K (Brüel & Kjær, Nærum, Denmark) type 4397 A accelerometer glued to

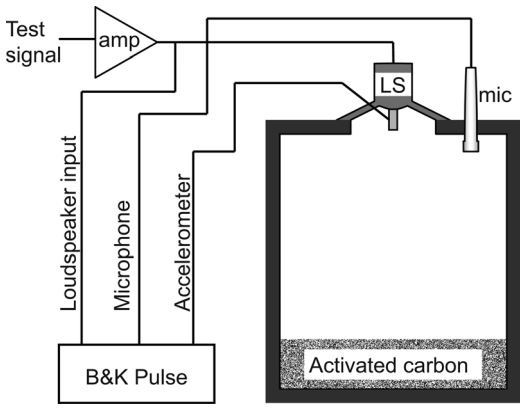

FIG. 4. Schematic of effective porosity and adsorption measurement apparatus.

the center of the dust-cap. The pressure was captured by a B&K type 4193 -L-004 low frequency microphone. A B&K PULSE 3560B front end recorded these quantities plus the voltage present at the loudspeaker's terminals. The amplifier's gain was set such that the signal amplitudes output by the compact disc player roughly corresponded to amplitudes of 1–4 V at the loudspeaker's terminals.

The bottom square plate is glued to the cylindrical sample holder, which had a diameter of 0.2519 m. The top plate was hermetically sealed using a semi-hardening adhesive. This allowed access to change samples, whilst maintaining an airtight seal during measurements. The sample holder was made from thick acrylic glass. To check for effects of temperature, thermocouple sensors were installed to monitor the temperature inside and outside the device. Slight variations in the internal temperature were observed, with a maximum range of 0.2 °C in any one measurement.

The stimuli stepped through pure tones at the 31 integer frequencies from 20 to 50 Hz in ascending order (some measurements used a wider frequency range). At each frequency the tone was played at four different amplitudes for 18 s each. This permitted sixteen 1 s measurements to be averaged while allowing 2 s for the system to settle. The data were windowed and a fast Fourier transform applied before the amplitude was extracted from the power spectrum and the phase from the transfer function between the pressure and displacement.

The activated carbon was sieved so as to achieve a grain size distribution between 0.3 and 0.42 mm. 1674 cm^3 of the material was selected using a large measuring cylinder and introduced as a layer approximately 3.4 cm thick at the bottom of the test chamber. A sample of 3 mm diameter lead shot was also measured, which had a volume of 500 cm^3.

A. Volume calibrations

Calibration was undertaken using two brass cylinders with identical dimensions—a diameter of 8.89 cm and a length of 15.23 cm, so the volume of each was 945.4 cm^3. The calibration formulations are derived from the following equation describing an ideal gas undergoing an adiabatic process:

$$PV^{\gamma} = \text{constant}, \tag{1}$$

where P is the pressure, V the air volume, and γ is the ratio of the specific heat capacities and is taken to be 1.4 for air. Introducing small acoustic perturbations Δp and ΔV in pressure and volume relative to the equilibrium states yields

$$\Delta V + \frac{\Delta p}{\gamma P} V = 0, \tag{2}$$

where $\Delta V = A_0 \Delta z$, with Δz being the displacement of the cone measured via the accelerometer, and A_0 is a constant. Three calibration measurements were used: $V = V_c$ (empty chamber), $V = V_c - V_b$ (one block present), and $V = V_c - 2V_b$ (two blocks present). With all the frequencies and amplitudes measured, this yields a vastly over-determined system of equations shown in the following, which was solved in a least-squares manner:

$$\begin{bmatrix} \Delta z_0 & \frac{\Delta p_0}{\gamma P} \\ \Delta z_1 & \frac{\Delta p_1}{\gamma P} \\ \Delta z_2 & \frac{\Delta p_2}{\gamma P} \end{bmatrix} \begin{bmatrix} A_0 \\ V_c \end{bmatrix} = \begin{bmatrix} 0 \\ \frac{\Delta p_1}{\gamma P} V_b \\ \frac{\Delta p_2}{\gamma P} 2V_b \end{bmatrix}, \tag{3}$$

where the integer subscripts applied to Δz and Δp indicate the number of blocks present in the chamber. Root mean square values are used for Δz and Δp, giving a chamber volume, V_c, of 14.83 liters and loudspeaker area, $|A_0|$, of 31.5 cm^2.

To confirm the linear least mean square fit is appropriate, a plot of Δp vs ΔV is made for the measured results and also for predictions based on Eq. (2). The plot is shown in Fig. 5. The measured pressures for the three non-adsorbing cases closely follow the predicted trends (minimum correlation coefficient 0.999 99). Measurements were also carried out on mineral wool, dry sand, and lead shot (graphs not shown), and all showed a linear trend as expected.

In Fig. 5, data have also been plotted for an activated carbon measurement. The measured pressure amplitudes are much lower than even the empty chamber. The curvature is due to the frequency dependence of both the effective porosity of the activated carbon and the displacement of the loudspeaker (for a constant driving voltage).

B. Effective porosity

To calculate the effective acoustic porosity of a sample, the process may be assumed to be adiabatic in the chamber but isothermal for air saturating the porous sample. The validity of this assumption will be clarified for each of the tested samples later. First consider the air volume above the sample $V_c - V_s$, where V_s is the volume of the porous sample. Introducing small acoustic perturbations Δp and Δv_1 in pressure and volume relative to the equilibrium states P and $V_c - V_s$ yields

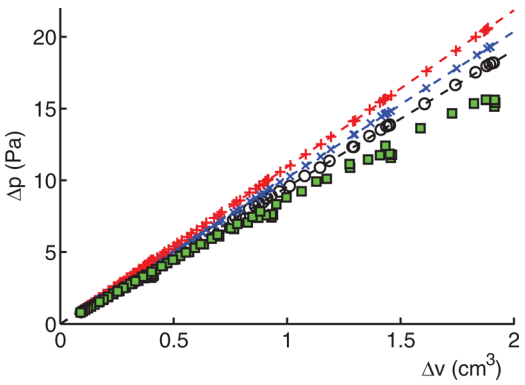

FIG. 5. (Color online) Acoustic pressure Δp vs volume displacement Δv for empty chamber (○); one brass block (×), two brass blocks (+), and activated carbon (■). Prediction lines using ideal gas law included for all cases except activated carbon.

$$\Delta v_1 + \frac{\Delta p}{\gamma P}(V_c - V_s) = 0. \tag{4}$$

The isothermal process for the air saturating the porous absorber is modeled using the ideal gas law,

$$PV = nRT, \tag{5}$$

where n is the number of moles of air present, R is the ideal gas constant (8.3145 J mol^{-1} K^{-1}), and T is the temperature (K). For now, adsorption is not explicitly modeled and the number of moles n is assumed constant. Perturbations of pressure Δp and volume Δv_2 of air inside the porous sample are related by

$$\Delta v_2 + \Delta p \frac{\varepsilon V_s}{P} = 0, \tag{6}$$

where ε is the material's porosity. Combining Eqs. (4) and (6), the following expression for the porosity is derived:

$$\varepsilon = -\frac{P}{V_s}\frac{\Delta V}{\Delta p} - \frac{1}{\gamma}\left(\frac{V_c}{V_s} - 1\right), \tag{7}$$

where $\Delta v = \Delta v_2 + \Delta v_1$ is calculated from the measured loudspeaker displacements Δz using the loudspeaker area A_0 determined from empty chamber measurements.

For samples with relatively large intergranular voids, the following equation, which assumes adiabatic behavior within the porous absorbent, is needed for some of the measurement bandwidth:

$$\varepsilon = -\frac{\gamma P}{V_s}\frac{\Delta V}{\Delta p} - \left(\frac{V_c}{V_s} - 1\right). \tag{8}$$

1. Lead shot

Measurements on lead shot were undertaken as part of the commissioning process for the apparatus. Unfortunately, for the sample used, the transition between isothermal and adiabatic behavior within the porous material probably lies within the measurement bandwidth. Measurements of the effective bulk modulus on smaller lead shot (1 mm diameter) using standard acoustic techniques[6] showed good correspondence between the expected isothermal value $(1/\varepsilon)$ up until 300 Hz, while at higher frequencies it approached the adiabatic value.[7] Assuming that the transition frequency between isothermal and adiabatic behavior is inversely proportional to the radius squared,[8] the 3 mm lead shot used in the activated carbon study is modeled as isothermal below 33 Hz and adiabatic above.

The effective acoustic porosity is calculated using Eqs. (7) and (8). The results are shown for an extended frequency range of up to 120 Hz in Fig. 6. The porosity will be inaccurate where there are significant energy losses because Δp will be lower than that expected from a naive application of the ideal gas equations. This might explain the increase in porosity above 60 Hz and consequently, subsequent analysis is carried out below this frequency.

Below 60 Hz, the effective porosity is amplitude dependent. This is most likely due to experimental errors when determining the chamber volume and loudspeaker area with the brass blocks. Consequently, an average of the porosity is calculated across all amplitudes and all frequencies from 20 to 55 Hz. This gives a porosity for the lead shot of (0.37 ± 0.03), which compares to 0.41 from directly weighing the sample and using the density of lead in a simple calculation.

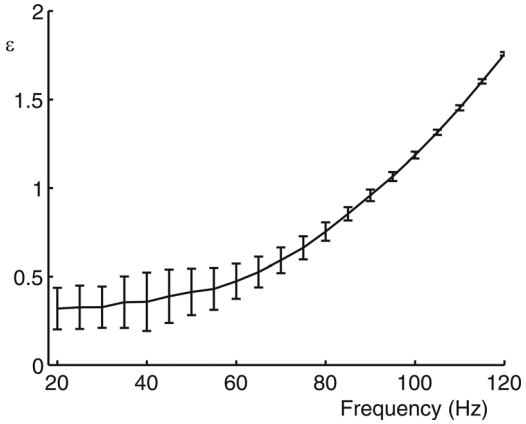

FIG. 6. Porosity of the lead shot sample averaged for four loudspeaker displacements vs frequency for an extended frequency range. Error bars are 95% confidence limits.

2. Activated carbon

Because carbon grains are smaller than lead shot particles it is assumed that the behavior within carbon is isothermal over the bandwidth of interest. The effective porosity for activated carbon is greater than one, as shown in Fig. 7(a). The number of moles of air that must be injected into a constant volume to achieve a given pressure change is larger than would be required if the material was not present and the chamber was just filled with air.

To demonstrate that adsorption could explain the low frequency behavior, a simple formulation is derived from the ideal gas law, Eq. (5), which explicitly models the moles adsorbed in the activated carbon,

$$\varepsilon V_s \Delta p + P \Delta v_2 = \Delta n RT, \tag{9}$$

where Δn quantifies the number of moles adsorbed and desorbed from the air saturating the activated carbon. To a first approximation, it is assumed that the number of moles adsorbed can be modeled as being linearly related to the acoustic pressure within the chamber $\Delta n = \xi \Delta p$. Combining Eqs. (9) with (4) gives

$$\Delta p = \frac{-P}{(V_C - V_S)/\gamma + \epsilon V_s - \xi RT}\Delta v. \tag{10}$$

Here the porosity value is taken to be 0.7 (taken from isotherm measurements given later in the paper). For each frequency, a plot of the amplitudes of Δp vs the amplitudes of Δv is made. (These are found to be linear for all frequencies with correlation coefficients varying between $-0.999\,995$ and $-0.999\,998$.) The gradient of a least-squares best fit line is used to estimate ξ, the number of moles adsorbed per unit

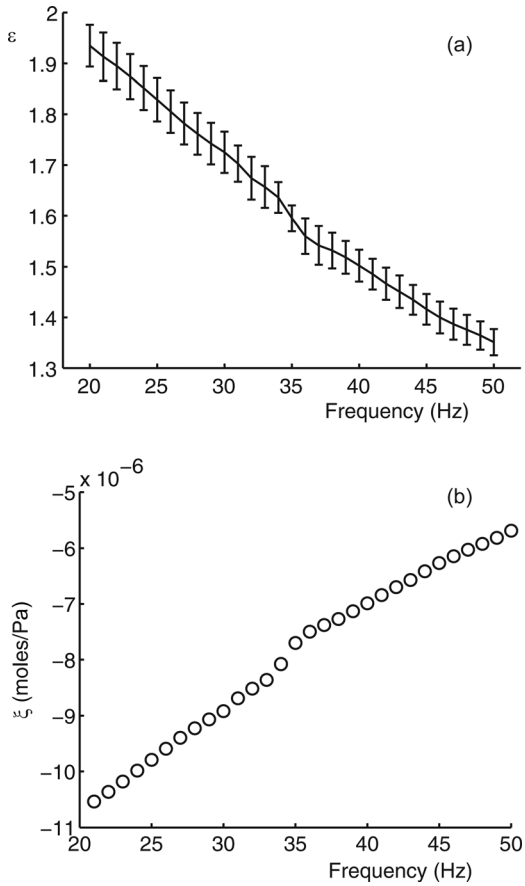

FIG. 7. (a) Effective porosity for activated carbon averaged over the four loudspeaker displacements; (b) number of moles adsorbed per unit of applied pressure, as a function of frequency for activated carbon.

of applied pressure, using Eq. (10). The mean temperature for the carbon measurement was 298.75 K. Figure 7(b) plots how ξ varies with frequency. Applying the same formulation to the lead measurement produces a mean value for ξ of $(-1.6 \pm 0.5) \times 10^{-9}$, 3 orders of magnitude smaller than the carbon results.

This provides evidence that adsorption could be affecting the behavior of sound waves interacting with the activated carbon for sound waves between 20 and 55 Hz and pressures between 104 and 118 dB. The number of moles adsorbed is greater at low frequencies, which is consistent with the idea that there is some time constant associated with sorption, making the effect on sound waves weaker at high frequencies.

A better analysis, however, examines the complex transfer function. The method has been used widely in chemical engineering to determine kinetic parameters of chemical reactions, sorption, and diffusion processes.[9] The volume of an air-filled chamber with the porous sample is perturbed periodically as $\Delta V e^{j\omega t}$, leading to air pressure variations of $\Delta p e^{j\omega t}$. The method exploits the relationship between the phase and the amplitude of the transfer function and the dynamics of the processes happening in the pores, where the transfer function $H = -V_a(\Delta p/\Delta V)/P$, where $V_a = V_c - V_s(1-\varepsilon)$ is the air volume at equilibrium and P atmospheric pressure. These processes are responsible for the rate at which the system returns to its equilibrium state.

It assumed that the activated carbon follows the Langmuir isotherm. The Langmuir isotherm is a common model for how the coverage of an adsorbed gas on a surface varies with the pressure of the gas at a fixed temperature. Assuming a single sorption process, the so-called real and imaginary response functions are defined as[9]

$$\mathrm{RRF} = \mathrm{Re}\left(\frac{H_0}{H} - 1\right), \tag{11}$$

$$\mathrm{IRF} = -\mathrm{Im}\left(\frac{H_0}{H} - 1\right), \tag{12}$$

where H_0 is the transfer function without sorption. $H_0 = \gamma$ if processes in both chamber and porous sample are adiabatic. If the gas is adiabatic in the air layer but isothermal inside the granular material, then $H_0 = \gamma/[1 + V_S\varepsilon(\gamma - 1)/V_a]$. As before, the former approximation will be used for the empty chamber while the latter will be assumed for the carbon sample. RRF and IRF have the following frequency dependence:

$$\mathrm{RRF} = \frac{K_s}{1+\Omega^2}, \tag{13}$$

$$\mathrm{IRF} = \frac{K_s\,\Omega}{1+\Omega^2}, \tag{14}$$

where $\Omega = \omega/k_r$ and k_r is adsorption relaxation frequency. The constant K_s is defined as the ratio of gas volume adsorbed/desorbed during one cycle $\Delta V = mRT(\partial n_s/\partial P)_{P=P_0}$ to the equilibrium gas volume V_a : $K_s = \Delta V/V_a$. Here m is the mass of air in the pores, R is the specific gas constant, and n_s is the concentration of the adsorbed molecules.

For a system with no sorption, both IRF and RRF should stay close to zero. If a single sorption process is present then the response should be like the inset shown in Fig. 8. The

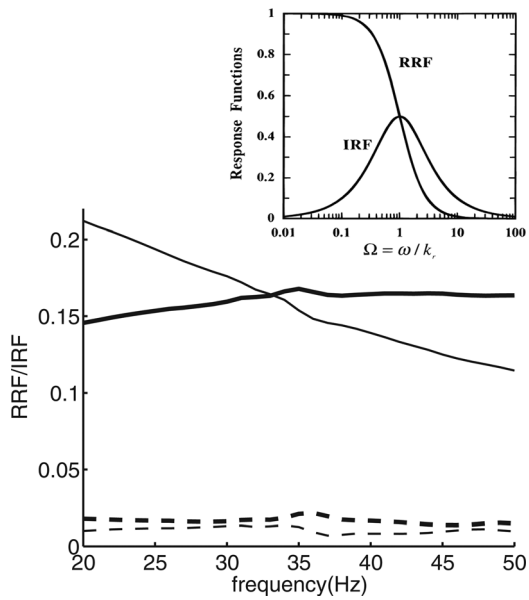

FIG. 8. ___, RRF activated carbon; _ _ _ _ _ _, RRF empty chamber; ___, IRF activated carbon; and _ _ _, IRF empty chamber. The top right inset is taken from Ref. 9.

RRF attains its maximum value of K_s at zero frequency and decreases with the frequency of perturbations, while IRF attains its maximum value of $K_s/2$ at $\omega = k_r$ and has a bell shaped dependence on frequency. RRF and IRF cross at $\omega = k_r$. At higher frequencies, IRF remains larger than RRF.

Response functions have been measured for the empty chamber and a chamber partially filled with activated carbon (Fig. 8). For the empty chamber the RRF and IRF remain relatively close to zero. Both response functions attain significantly higher values for a chamber with activated carbon in it. The measured RRF and IRF cross at a certain frequency (≈33 Hz) and the IRF remains bigger than RRF at higher frequencies. Moreover, RRF value decreases with frequency. These features are in agreement with those predicted by the model. However, in general the measured response functions do not behave exactly as the theoretical ones. At least three reasons for the discrepancies can be suggested: (1) Sorption in the activated carbon does not follow the Langmuir isotherm; (2) the sorption could be accompanied with Fickian gas diffusion into the micropores of the particles,[9] and (3) viscous friction between the air and the surface of carbon particles leads to some extra energy losses, which are not accounted for in the model.

IV. FURTHER IMPEDANCE TUBE MEASUREMENTS

The energy absorption of activated carbon alone (not in a resonant structure) was quantified by a series of measurements in the low frequency impedance tube. The granular activated carbon was loosely packed at the bottom of the sample holder.

Figure 9 shows measured absorption coefficients for a range of depths of activated carbon showing that the absorption increases with sample thickness as expected for a porous absorber. The magnitude of low frequency absorption is perhaps more surprising. For example, at 100 Hz, a 2.4 cm thick sample has an absorption coefficient of about 0.24. Control measurements on the sand sample of the same sample depth produced an absorption coefficient of only 0.04 at the same frequency. Since the granular packing of the two materials might be assumed to be similar, this suggests an addition phenomenon, such as sorption, causing additional absorption.

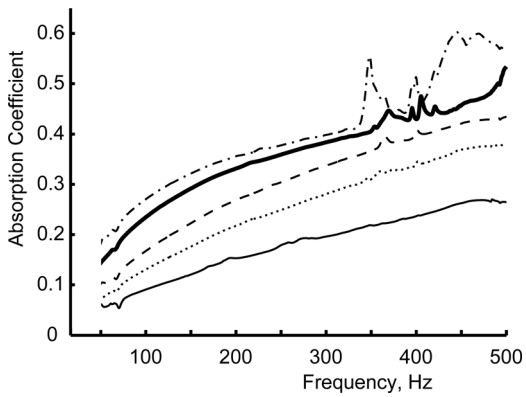

FIG. 9. Absorption coefficient measured in the impedance tube for activated carbon for various thicknesses: ___, 8.1; ....., 12.1; _ _ _ _, 16.2; ___, 24.2; and _._._, 32.4 mm.

Furthermore, other porous materials more commonly used as acoustic absorbers and of similar thickness have absorption coefficients smaller than that observed for activated carbon. For example, Castagnede *et al.*[10] measured absorption coefficients of about 0.03 at 100 Hz for two samples of comparable thickness, one made from plastic foam, the other mineral wool. Horoshenkov *et al.*[11] measured average absorption coefficients for three different porous absorber samples of similar thickness. For reticulated foam and fiberglass the absorption coefficients at 100 Hz were 0.05 and 0.08 (a third sample is ignored because it had a distinct structural resonance).

Figure 10 shows the surface impedance for one of the activated carbon samples and the sand sample of the same thickness. The results indicate that the additional absorption provided by the activated carbon is caused by a decrease in the magnitude of the capacitive reactance. The differences in surface resistance are smaller and tend to move the activated carbon further from the characteristic impedance of air compared to sand and so would act to reduce the absorption coefficient.

V. ISOTHERM PRESSURE COMPOSITION MEASUREMENTS

A series of isotherm measurements were undertaken to further examine the sorption. They also characterize the physical properties of the activated carbon sample showing strong effects on low frequency sound. Unlike the measurements presented previously, these were carried out with applied pressures far in excess of those occurring in typical audible sound waves, because they exploit standard apparatus used for sorption measurements.

A. Method and porosity measurements

Adsorption isotherms were obtained using the intelligent gravimetric analyzer shown in Fig. 11. The instrument measures the mass change of a given solid sample upon solid/gas interactions in a sealed chamber at set temperatures and pressures. The pressure transducers (*M* in Fig. 11), have a

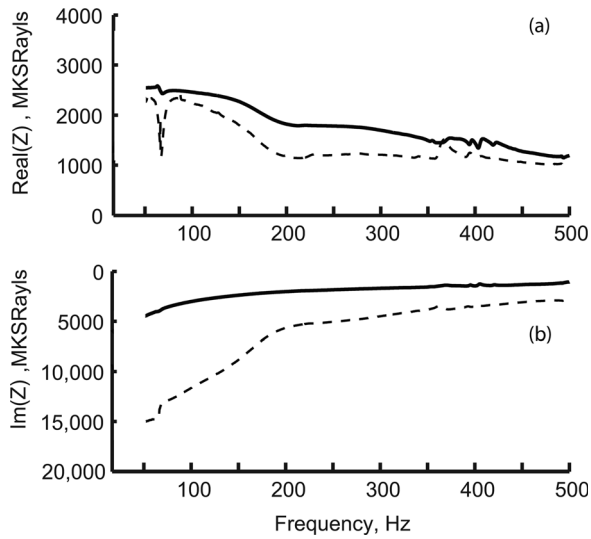

FIG. 10. Impedance of ___, activated carbon and _ _ _ _, sand both 2.42 cm thick measured in the impedance tube. (a) Real, (b) imaginary.

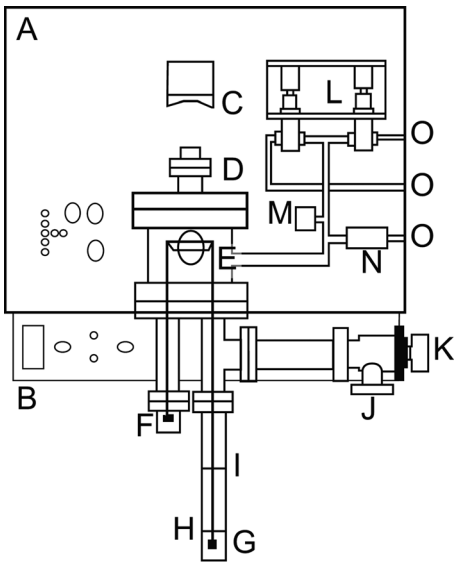

FIG. 11. Schematic of intelligent gravimetric analyzer: A, thermostated enclosure; B, external electrical connections; C, thermoregulator; D, vacuum-pressure assembly; E, microbalance movement; F, tare pan; G, sample pan; H, temperature sensor(s); I, adjustable baffles; J, vacuum port; K, vacuum-pressure isolation valve; L, pressure controller/gas feed; M, pressure transducer(s); N, pressure relief valve; O, external ports (gas admit/exhaust/vent).

measurement range between 10^{-6} mbar and 20 bar. The microbalance (E) holds a maximum sample mass of 5 g, with a measurement accuracy better than 5 μg. The temperature of the sample can be increased using a furnace or reduced using a liquid nitrogen bath.

Before measurements were performed, the activated carbon sample was outgassed to evacuate any adsorbed substances. This is achieved by reducing the pressure in the sample chamber to near vacuum (10^{-6} mbar) by attaching the outlet (J) to a vacuum pump, and raising the temperature of the system over a time period ($\approx$12 h) long enough to ensure the evaporation of non-gaseous adsorbed substances; this is done until the mass of the sample stabilizes.

For the isotherm measurements, a gas is introduced through the inlet valve (O). Changes in the equilibrium sample mass are measured as the pressure in the system is increased in steps from near vacuum to a predetermined saturation pressure value. Constant temperature is maintained. In addition, the time taken for the mass of the sample to reach equilibrium is measured. Next, the pressure is reduced from the saturation value toward vacuum to investigate desorption. This set of measurements is known as the adsorption isotherm.

The effect of buoyancy needs to be accounted for because it produces an upward force exerted by the gas on a fully submerged activated carbon sample and affects the measured weight. For that reason, a helium isotherm was measured at 373.2 K. This allows the evaluation of the sample's specific density, i.e., the apparent density of the solid part of the activated carbon plus the volume not accessible to helium. Helium is used because little will adsorb onto the activated carbon, as it is an inert gas with only a small polarizability.

During the buoyancy measurement, the mass of the sample was seen to increase very slightly for very low relative pressures. For that reason, the buoyancy and solid density were determined from experimental data at higher pressures, where the effect of buoyancy followed expected patterns more closely. Two isotherms were measured, which gave solid density results of $\rho_s = 1.85\,\mathrm{g\,cm^{-3}}$ and $\rho_s = 1.66\,\mathrm{g\,cm^{-3}}$. The latter result was evaluated at slightly higher pressure. (These values are lower than the nominal solid density of carbon given by the manufacturer of the sample, $2.2\,\mathrm{g\,cm^{-3}}$.)

The bulk density found by weighing 1 liter of the material was $0.525\,\mathrm{g\,cm^{-3}}$. Using the dry mass of the carbon sample (42.874 mg), when $\rho_s = 1.85\,\mathrm{g\,cm^{-3}}$, a porosity of 0.716 results. If $\rho_s = 1.66\,\mathrm{g\,cm^{-3}}$, the porosity becomes 0.684. The average is 0.70.

B. Hysteresis and humid air

Adsorption isotherms for nitrogen and humid air at room temperature were then investigated; these are shown in Fig. 12. For humid air, the presence of water vapor near its condensation point causes its phase to change from a gaseous state to a liquid one as the pressure is increased. The humid air isotherm reveals significant hysteresis in the sorption cycle, caused by the differences between the adsorption and desorption rates of water vapor molecules. The amount of adsorbed air molecules, at any given pressure, is always greater during desorption than during adsorption.

In contrast, the isotherm for dry nitrogen shows the same rate of adsorption and desorption, because no condensation occurs in the pores over the measured pressure range. This difference in hysteresis behavior is made clear in the relaxation times summarized in Table II.

1. Determination of sorption rate constants

Mass changes for an activated carbon sample immersed in humid air were measured as a function of a dynamic change in the pressure; Fig. 13 shows the results for one such test. The increase in mass as function of time and pressure was calculated, as well as the amount of adsorbed

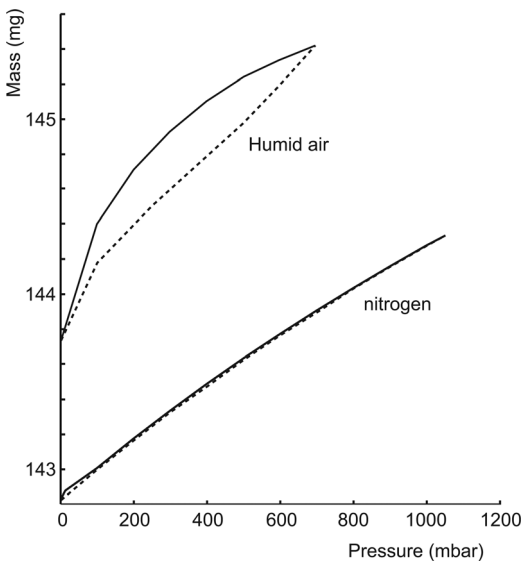

FIG. 12. Sorption isotherms for humid air and nitrogen at 293.2 K ----, adsorption and ——, desorption.

TABLE II. Relaxation times for adsorption and desorption as evaluated from the sorption isotherm with humid air at 293.2 K.

Adsorption		Desorption	
Pressure (mbar)	Relaxation time (s)	Pressure (mbar)	Relaxation time (s)
1.222	0	697.31	0
100.11	822 ± 27	598.43	14.8 ± 1.7
250.05	112 ± 13	501.16	25.0 ± 1.1
499.55	63.6 ± 1.8	399.45	39.8 ± 1.0
599.24	65.5 ± 1.5	298.41	45.5 ± 2.0
697.31	62.9 ± 2.5	199.66	87.6 ± 7.2
		99.028	208.5 ± 5.3
		1.357	62.35 ± 0.94

substance for each unit mass of the sample (known as the adsorption rate constant).

It was found that during compression, the initial rate of change in the sample mass is of the order of 5.5×10^{-5} mg s^{-1}. Over a longer time period, the rate of adsorption is expected to reduce as the activated carbon becomes saturated and the sorption process reaches equilibrium. By taking an average of the mass increase at each compression pressure, i.e., the molar mass adsorbed, and relating it to the total mass of the sample, it is possible to derive the molar adsorption and desorption rates. For a pressure change of 100 mbar (10 kPa), the molar adsorption and desorption rate constants were found to 0.199 and 0.165 μmol g^{-1}, respectively.

By investigating the lag between a pressure compression being applied and the subsequent increase in mass, the adsorption and desorption response times were obtained. These were found to be 2.1 and 38.4 s for adsorption and desorption, respectively, and again demonstrate the presence of hysteresis. The long desorption relaxation time is associated with the slow kinetics of water vapor adsorption, which delay the return to the equilibrium mass, since water vapor molecules continue to adsorb during rarefaction.

C. The activated carbon tested

Isotherms also allowed the activated carbon sample to be characterized. The 77 K nitrogen uptake isotherms were used to obtain the surface area via a Brunauer–Emmett–Teller (BET) analysis,[12] and the micropore and mesopore distributions using the methods of Dubinin–Astakhov[13] and Brunauer–Joyner–Halenda,[14] respectively. The activated carbon was found to be type I,[15,16] which is associated with physical adsorption in materials containing extremely fine pores. The Dubinin–Astakhov analysis showed that the concentration of mesopores (2 nm < width < 50 nm) is very small.

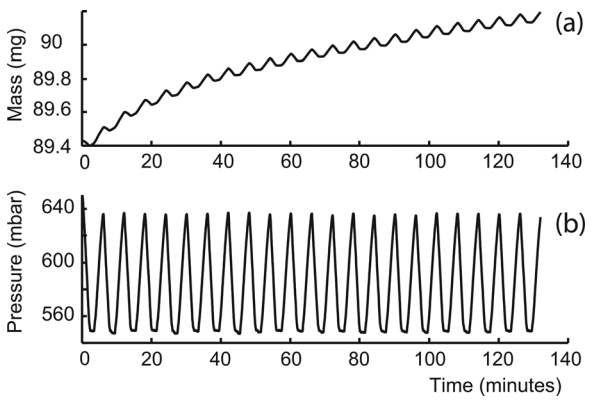

FIG. 13. (a) Mass change in activated carbon sample over time as (b) pressure is dynamically changed in the intelligent gravimetric analyzer.

The largest distribution of pores is micropores, which have widths between 0.5 and 1 nm, with 0.7 nm being the most common. This is equal to twice the separation between the graphene layers forming the structure of the activated carbon (0.34–0.35 nm). The BET analysis showed that in the micropores (width < 2 nm) the surface area density was (968 ± 47) $m^2 g^{-1}$. However, under uncontrolled environmental conditions such pores might be expected to be completely saturated with adsorbed substances—in particular, condensed water vapor—which makes them ineffective as far as sorption is concerned and unlikely to have a significant effect on acoustic wave propagation. The effective volume in each of the pore scales was also estimated using a method proposed by Fuller.[17] For the micropores, a volume of 651 cm^3 is available for each gram of activated carbon (99.2% of the total volume available for adsorption), while for macropores only a very small volume of 5.0 cm^3/g is available.

Analysis of scanning electron microscope images was used to determine further information concerning the macropores and intergranular voids.[18,19] The distribution of macropores (width > 50 nm) in the carbon grains is largest for pore widths between 0.17 and 0.28 μm. The granular activated carbon was sieved between 0.30 and 0.42 mm grain diameter, resulting in intergranular voids with widths concentrated around ~0.25 mm, which form up to 45% of the total surface area of the sample.

VI. DISCUSSIONS AND CONCLUSIONS

The absorption coefficient of activated carbon was measured in an impedance tube between 50 and 500 Hz and found to be larger than expected for other common porous materials. The excess absorption is due to reductions in surface reactance rather than changes in surface resistance. The reduced reactance can also account for the changes in resonant frequency observed with Helmholtz resonators with activated carbon in their backing volume. Above (roughly) 150 Hz, the results from the Helmholtz resonators can be explained by the isothermal behavior of the granular material. Below 150 Hz, however, another mechanism is needed to explain the behavior. The reduction in resonant frequency is largest at low frequency, which is consistent with a phenomenon requiring time to take effect, as would be the case with sorption.

Measurements to determine the effective porosity using low frequency sound waves (104–118 dB and 20–55 Hz) produced values greater than one for activated carbon. A simple adaption of the ideal gas law, to include the number of moles adsorbed as proportional to the applied acoustic pressure, was used to model the measurements. A preliminary study into using sorption kinetics and formulations based on the

Langmuir isotherm showed some promise, but further work is needed to determine why the measured responses differ from theoretical expectations in some respects.

A series of adsorption isotherms were measured. When nitrogen was used as the adsorbing gas at room temperature the rates of adsorption and desorption were the same. In contrast, when humid air was used, water vapor condensation causes a difference between the rates of adsorption and desorption and hysteresis in the sorption cycle is observed. Water vapor condensation and evaporation might therefore explain the difference in surface resistance between the activated carbon and sand measured in the impedance tube. However, as the isotherm measurements were carried out at different pressures and temperature conditions compared to the impedance tube measurements, there is insufficient evidence to be sure of this conclusion.

The aim of this study was to determine whether sorption significantly affects the propagation of sound through activated carbon at low frequency. The results gathered are consistent with this hypothesis, but the conclusive proof of what causes the change in surface reactance remains elusive. It is still conceivable that other phenomena, such as multi-scale porosity, slip flow,[20] or gas diffusion, might play a part. Whatever the cause, this study has confirmed that activated carbon can be used to change the compliance of enclosures, and to enable higher absorption at a lower frequency than would otherwise be expected from conventional porous absorbers.

[1]J. R. Wright, "The virtual loudspeaker cabinet," J. Audio Eng. Soc. **51**, 244–247 (2003).

[2]ISO 10534-2: *Acoustics—Determination of Sound Absorption Coefficient and Impedance in Impedance Tubes. Part 2: Transfer Function Method* (ISO, Geneva, 1998).

[3]T. J. Cox and P. D'Antonio, *Acoustic Absorbers and Diffusers* (Taylor & Francis, London, 2009), pp. 77–78.

[4]Y. Cho, "Least squares estimation of acoustic reflection coefficient," Ph.D. dissertation, University of Southampton, U.K., 2005.

[5]A. Selamet, M. B. Xu, and I.-J. Lee, "Helmholtz resonator lined with absorbing material," J. Acoust. Soc. Am. **117**(2), 725–733 (2005).

[6]R. Venegas and O. Umnova, "Acoustic properties of double porosity granular materials," J. Acoust. Soc. Am. **130**(5), 2765–2776 (2011).

[7]R. Venegas, "Microstructure influence on acoustical properties of multi-scale porous materials," Ph.D. dissertation, University of Salford, U.K., 2011.

[8]C. Boutin and C. Geindreau, "Periodic homogenization and consistent estimates of transport parameters through sphere and polyhedron packings in the whole porosity range," Phys. Rev. E **82**, 036313 (2010).

[9]S. C. Reyes, J. H. Sinfelt, G. J. DeMartin, R. H. Ernst, and E. Eglesia, "Frequency modulation methods for diffusion and adsorption measurements in porous solids," J. Phys.Chem. B **101**, 614–622 (1997).

[10]B. Castagnede, A. Moussatov, D. Lafarge, and M. Saeid, "Low frequency in situ metrology of absorption and dispersion of sound absorbing porous materials based on high power ultrasonic non-linearly demodulated waves," Appl. Acoust. **69**(7), 634–648 (2008).

[11]K. V. Horoshenkov, A. Khan, F. X. Bécot, L. Jaouen, F. Sgard, A. Renault, N. Amirouche, F. Pompoli, N. Prodi, P. Bonfiglio, G. Pispola, F. Asdrubali, J. Hübelt, N. Atalla, C. K. Amédin, W. Lauriks, and L. Boeckx, "Reproducibility experiments on measuring acoustical properties of rigid-frame porous media (round-robin tests)," J. Acoust. Soc. Am. **122**, 345–353 (2007).

[12]S. Brunauer, P. H. Emmett, and E. Teller, "Adsorption of gases in multimolecular layers," J. Am. Chem. Soc. **60**, 309–319 (1938).

[13]M. M. Dubinin and V. A. Astakhov, "Description of adsorption equilibria of vapors on zeolites over wide ranges of temperature and pressure," Adv. Chem. Ser. **102**, 69–85 (1970).

[14]E. P. Barrett, L. G. Joyner, and P. P. Halenda, "The determination of pore volume and area distributions in porous substances. I. Computations from nitrogen isotherms," J. Am. Chem. Soc. **73**, 373–380 (1951).

[15]S. J. Gregg and K. S. W. Sing, *Adsorption, Surface Area and Porosity*, 2nd ed. (Academic, London, 1982), pp. 1–303.

[16]S. Brunauer, L. S. Deming, W. E. Deming, and E. Teller, "On a theory of the van der Waals adsorption of gases," J. Am. Chem. Soc. **62**, 1723–1732 (1940).

[17]J. W. Hassler, *Activated Carbon* (Chemical Publishing Company, New York, 1963) pp. 1–397.

[18]L. Wojnar, *Image Analysis, Applications in Materials Engineering* (CRC Press, Boca Raton, FL, 1998), pp. 1–256.

[19]J. Serra, *Image Analysis and Mathematical Morphology* (Academic, Orlando, 1983), pp. 1–610.

[20]O. Umnova, D. Tsilklauri, and R. Venegas, "Influence of boundary slip on acoustical properties of microfibrous materials," J. Acoust. Soc. Am. **126**, 1850–1861 (2009).